Use of the S- alpha diagram for representing tokamak equilibria in profile modification research

USE OF THE S-α DIAGRAM FOR REPRESENTING TOKAMAK EQUILIBRIA IN PROFILE MODIFICATION RESEARCH

H. TAKAHASHI, M.S. CHANCE, C.E. KESSEL,
B. LeBLANC, J. MANICKAM, M. OKABAYASHI
Princeton Plasma Physics Laboratory,
Princeton University,
Princeton, New Jersey,
United States of America

ABSTRACT. In tokamak research involving plasma profile modification, it is proposed to represent a plasma equilibrium state as a trajectory in a diagram of shear and dimensionless pressure gradient commonly known as the S-α diagram. The method is a natural way of exhibiting local variations of the shear and pressure gradient and their interrelationship. A distinct equilibrium trajectory pattern may be associated with a set of experimentally observed phenomena, such as the level and kind of MHD activity or confinement, or with theoretically predicted properties such as the stability. When many qualitatively different trajectory patterns are identified with a set of observed or predicted characteristics, the diagram will serve as a tool for cataloguing the presently achievable plasma states as well as desired target states through 'pattern recognition'. Furthermore, types of trajectory changes produced by various profile modification techniques can also be represented in the same diagram. The method will help construct a desired state, starting from a given experimental state using profile modification techniques. It is demonstrated, using PBX-M experiments as examples, that distinct trajectory patterns can be associated with different operational regimes, and that some profile modification techniques and types of MHD activity produce characteristic trajectory changes.

1. INTRODUCTION

An important task in present fusion research is to develop methods for producing a plasma with improved MHD stability and confinement. The current and pressure profiles are among the important properties of a plasma that influence its equilibrium, stability and confinement. Various techniques for controlled profile modification and their efficacy and consequences for MHD stability and confinement are being studied at many institutions. Experimental techniques[1] include external shaping (e.g. ellipticity, triangularity and/or indentation) [1, 2], the skin effect (rapid I_p rampup or rampdown) [3-6], beam driven and bootstrap currents [7, 8], pellet injection [9], ion Bernstein wave heating (IBWH) [10] and lower hybrid current drive (LHCD) [11, 12]. Theoretical studies are also being pursued, both in conjunction with these experiments and as part of design and performance predictions for future devices.

In all research efforts involving profile modification, it becomes necessary to characterize the nature of profiles and relate it to observed or predicted properties of the plasma, for example to its MHD activity, stability or confinement. Quantitative characterization of profiles is typically made through the use of global parameters, such as the internal inductance, ℓ_i, for current profiles, or the pressure peaking factor, $p_f \equiv p_0/\langle p \rangle$, where p_0 and $\langle p \rangle$ are the peak and volume averaged pressures, respectively. These parameters are integral moments of profile functions and have the advantage of being simple. Such a method of characterization has successfully led to delineation of operating regimes of existing tokamaks and to development of design criteria for future devices.

Stability and confinement often depend on local profile characteristics. Furthermore, profile features are often only meaningful with respect to another profile's features. For example, a pressure profile considered 'peaked' for a certain current profile may not be regarded as being peaked for another current profile. Integral moments obscure local variations and say little about their interrelationship. There is the need for methods to adequately describe a local profile characteristic in relation to another. Such methods should be standardized or widely

[1] Representative references are cited here. Profile modification is a topic of current interest, and up to date literature can be found in the proceedings of major international conferences on plasma physics and nuclear fusion.

used so that comparisons can be made easily among experiments and theoretical studies.

The shear and the dimensionless pressure gradient are among the parameters important for stability. A natural way of exhibiting their *local variations* and *interrelationship* is to borrow the concept of the S–α diagram, in which the shear S and the dimensionless pressure gradient α are parametrically depicted as functions of the poloidal flux ψ. The S–α diagram has been in use for many years, primarily for the purpose of showing the stability boundary of high-n ballooning modes (n is the toroidal mode number). In this paper, however, we want to use the diagram for characterizing the plasma equilibrium. The question of stability will naturally arise, but only as a qualitative notion, and we are not specifically limiting our attention to the high-n ballooning modes. Depicting an equilibrium, whether it is a representation of an experimental plasma or a theoretical model, as a trajectory in the diagram, together with the locations of some rational surfaces, will serve the purpose of showing both the local variations of the shear and the pressure gradient and their interrelationship. Observed or predicted plasma properties will then be associated with the trajectory.

Since these quantities are distributed across the plasma and cannot be represented by a single number, we propose the use of 'pattern recognition'. Qualitatively or topologically distinguishable features of a curve can be recognized as being frequently associated with a set of experimentally observed plasma characteristics. We can then 'catalogue' different combinations of current and pressure profiles through pattern recognition. Equilibria theoretically predicted to be desirable for a particular purpose can also be characterized in the same manner. Furthermore, the capability of individual profile modification techniques can also be represented in the same diagram. We would then have an effective tool to help construct a desired plasma state out of the present state using profile modification techniques. These potential areas of application are elaborated further in the following three paragraphs.

Pattern recognition is useful for characterizing different operating regimes of a tokamak. It is also useful for comparing different devices. Like other methods of presentation based upon the poloidal flux, the S–α representation is independent of the plasma shape and size, and is a suitable means of comparing equilibria from different devices and to extract features common or specific to their operating regimes. In such comparisons the plasma shaping ability of a device is implicit as an available technique to alter the S–α pattern. For example, H-mode regimes from two devices having distinct trajectories and different performance characteristics would naturally prompt investigations of the origin of the differences. Such differences are often not readily discernible from examinations of individual current and pressure profiles. The use of a standardized method of representing equilibria will help to promote such comparisons.

In theoretical works on the β limit set by MHD stability, optimized equilibria have been found that were thought to be advantageous in achieving a specific goal, for example reaching a second stable regime. The S–α diagram has sometimes been used to describe these equilibria [13–16][2], although not specifically for comparing trajectory patterns or associating them with MHD characteristics. Different definitions of S and α used in these publications also made pattern comparisons difficult. In the areas of performance prediction of future devices, optimized equilibria have been extensively analysed for their stability characteristics. These equilibria were often referred to by such terms as INTOR-like [17] or ITER-like [18] plasmas, and were usually characterized through explicit specification of pressure and current (or safety factor) profiles. These theoretical works provide a 'target state', which various profile modification tools may strive to achieve. Representation of these target equilibria in a standardized S–α diagram facilitates easy comparisons among them, as well as with presently achievable equilibria.

Systematic characterization of the capability of profile modification tools in altering the equilibrium trajectory in the S–α diagram is also needed. For example, pellet injection may change the equilibrium trajectory from one type of pattern to another, but the degree of modification may depend upon the pellet size and speed. It would also be useful to know what kind and magnitude of changes in the equilibrium trajectory can be achieved by LHCD using a different parallel refractive index ($n_{\parallel}$) spectrum. Efforts to modify the 'present state' into a 'target state' can be hampered by an MHD instability that may intervene between the states. But limitations set by various transport processes will also be important: wave or beam penetration and localization, and magnetic, heat or particle diffusion. The hypothesis that the present state can be transformed into a particular target state must therefore be verified through experimentation. The knowledge of the present and target states and of the capability of profile modification tools, all expressed in a *standardized* S–α diagram,

[2] The points representing the equilibrium in the small figures in Fig. 4 of Ref. [16] can be connected to form a trajectory.

will help to construct a hypothesis and to conduct experiments to prove (or disprove) it.

We will demonstrate in this paper that operational regimes of a tokamak exhibiting different MHD characteristics can possess qualitatively distinct curves in the S-α diagram. We suggest that it may be worth while to explore whether any association can be found between the trajectory pattern and confinement characteristics, although we offer no examples for it in this paper. Specific experimental examples are taken from the PBX-M tokamak project [19]. A major goal of the project is to find ways to produce plasmas with improved MHD stability and confinement through control of current and pressure profiles. Specifically, we want to study the nature of MHD activity and other phenomena causing the β limit, to find ways to overcome it through profile manipulation, and to achieve second stability with respect to high-n ballooning modes. To date, the main profile modification techniques have been external shaping (indentation, or bean shaping, in particular), the skin effect, beam driven current and pellet injection. When we apply one or more of these techniques, we find that profiles are indeed modified. But these techniques are crude as a means of *controlling* profiles. In the near future, IBWH and LHCD will also be added, which are expected to allow more localized profile manipulation. As an illustration, the diagram is used to characterize three different operating regimes of the PBX-M tokamak: an H-mode regime with high β_p (poloidal β), an L-mode regime with high $\langle\beta_t\rangle$ (volume averaged toroidal β) and a pellet injection regime.

2. THE S-α MAP REPRESENTATION OF EQUILIBRIUM

An example diagram, here referred to as the S-α 'map', is shown in Fig. 1. The shear and pressure gradient parameters in this paper are defined[3] as

$$S(\psi) \equiv (2v/q)(dq/d\psi)(d\psi/dv) \quad (1)$$

$$\alpha(\psi) \equiv (-2\mu_0)(dp/d\psi)(dv/d\psi)\sqrt{v/2\pi^2R} \quad (2)$$

where ψ is the poloidal flux. (The poloidal field vector is defined by $\vec{B}_p \equiv \nabla\phi \times \nabla\psi$, where φ is the toroidal angle co-ordinate.) The volume within a flux surface defined by ψ is v(ψ). The reference major radius (magnetic axis in this paper) is R, the pressure is p(ψ) and the safety factor is q(ψ). Each of the two solid curves, labelled (A) and (B), is a parametric representation of S(ψ) and α(ψ) for an equilibrium, as the parameter ψ is varied from its value on the magnetic axis ('x' at the origin of the diagram) to the value at the plasma edge ('a' or 'b' on the vertical axis). The last segment of each trajectory, representing changes between the last two flux surfaces, is omitted for the clarity of presentation. Numerals embedded in the curves mark locations of integer q values and are an important part of the S-α map. Patterns traced by curves (A) and (B) are typical of high β_p and high $\langle\beta_t\rangle$ plasmas in PBX-M, respectively (see below). These patterns are qualitatively different from each other and suggest that 'pattern recognition' may be a useful tool to catalogue discharges in different regimes.

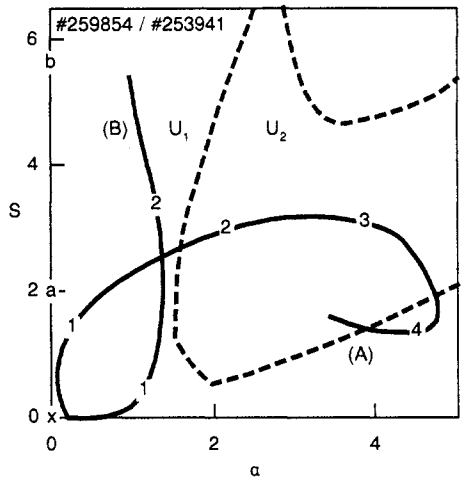

FIG. 1. The S-α map: Trajectories (solid curves) representing equilibria, with locations of integer q values indicated, for an H-mode plasma with high poloidal β (A) and an L-mode plasma with high toroidal β (B). The broken curves U_1 and U_2 are representative high-n ballooning stability boundaries of the H-mode equilibrium (for flux surfaces with q = 1.7 and 3.4, respectively). Curves (A) and (B) are obtained from PBX-M shots #259854 and #253941, respectively.

The traditional use of the S-α diagram is to represent the high-n ballooning mode stability boundary. Depicted also in Fig. 1 are the stability boundaries for high-n ballooning modes for two representative flux surfaces of the equilibrium described by trajectory (A). The curve U_1 is the stability boundary (unstable in the 'upper right corner' within the curve) for a point on the trajectory having q = 1.7. Similarly, the curve U_2 is for a point with q = 3.4. There have been attempts to combine the representation of both equilibrium trajectory and stability boundary in the same diagram.

[3] These definitions, which reduce, in the large-aspect-ratio limit, to forms originally used by Connor et al. [20], have been in use at General Atomics and Princeton Plasma Physics Laboratory.

For example, a way to construct a 'universal' stability boundary applicable to all flux surfaces of an equilibrium has been devised [14]: for the i-th flux surface with an associated value of S_i there is a pair of values, $\alpha_i(1)$ and $\alpha_i(2)$, that demarcates the unstable region from the first and second stable regions, respectively, and the two points in the diagram $(S_i, \alpha_i(1))$ and $(S_i, \alpha_i(2))$ can be traced out for all values of 'i'. The stability boundary in this representation is, however, found by varying α alone while holding S constant, and is a pair of points (or a single point) in the S–α plane for each flux surface. In contrast, the boundary in a more recently prevailing representation is obtained by varying both S and α, and is a curve in the S–α plane for each flux surface. A complex three-dimensional stability boundary has also been used (the third dimension representing the flux surfaces) together with a space curve depicting the underlying equilibrium [21]. A method of constructing an 'almost universal' stability boundary in a two-dimensional diagram has also been devised [22] which relies on scaling, or 'distorting', of S and α axis.

In promoting the use of the S–α diagram for representing an equilibrium, rather than for depicting the stability boundary, we are in part motivated by practical considerations. While the computation of stability criteria itself can be precise, it is often difficult under practical circumstances to establish unambiguously a theoretical representation of an actual plasma. Such imprecision arises often from the lack of experimental knowledge sufficient to define a theoretical model. For example, a stability analysis based on theoretical calculations with one value of wall distance may lead to kink stability, while calculations with a slightly different distance would lead to instability. Yet, in many practical situations, the wall shapes are so complex that the wall distance cannot be readily defined. On the one hand, a stability calculation will yield under such circumstances a black and white answer to an ill defined problem. On the other hand, we believe that there are pattern characteristics of the equilibrium S–α trajectory that can be recognized and differentiated. Such pattern characteristics can also be associated with observed or predicted plasma properties.

3. OPERATING REGIMES

Equilibria discussed in this paper are constructed on the basis of experimental data from three different operating regimes in the PBX-M tokamak: an H-mode regime with high β_p, an L-mode regime with high $\langle\beta_t\rangle$, and a pellet injection regime. These experimental regimes are described here to show that they exhibit different MHD and confinement characteristics. The description will be brief, because the principal purpose of this paper is to illustrate the usefulness of the diagram, not to report experimental achievements of the tokamak. More complete descriptions of the high β_p and high $\langle\beta_t\rangle$ regimes can be found in Ref. [23].

The high β_p regime is produced primarily by *shaping*. The plasma state in this regime is often produced in discharges exhibiting a so-called β collapse process[4] in which β_p rises, saturates and falls. In these 'β collapse discharges', the plasma undergoes a transition to the H-mode during an early phase of neutral beam injection (NBI) heating, and the plasma stored energy initially rises strongly with time. The β_p also reaches a high value. However, the stored energy and β_p reach a peak or saturate (i.e. stay steady over a period comparable to, or longer than, the confinement time), and then decrease, presumably owing to MHD activity, in spite of a steady heating power delivered by NBI heating. The plasma states reached at (or near) the peak or during the saturation phase of these discharges are in the high β_p regime. Plasmas in this regime have a moderate indentation ($\iota \sim 0.15$), ellipticity ($\kappa \sim 1.9$) and triangularity ($\delta \sim 0.5$). These H-mode, quasi-steady plasma current ($I_p \sim 320$ kA) discharges are characterized by a high β_p value (~ 2), a low Troyon–Sykes parameter ($\beta_{TS} \equiv I_p/(a_{mid}B_{\phi 0}) \sim 1.2$ MA/m·T) and a moderate g factor ($g \equiv \langle\beta_t\rangle/\beta_{TS} \leq 3.0\%\cdot m\cdot T/MA$, where $\langle\beta_t\rangle$ is the volume averaged toroidal β in %). These plasmas are in the first stability region, although some flux surfaces may be close to the second stability region with respect to high-n ballooning modes [23]. This regime has the advantage of a quasi-steady-state plasma current and is presently considered as a prime candidate for achieving second stability using current profile modification techniques. Ironically, however, these discharges have much global MHD activity after β_p reaches its peak or saturation. Only sawteeth are observed in the rise phase, but frequent fishbones and small edge localized modes (ELMs) [26] are seen in the saturation phase, and continuous global modes (mostly with n = 1, but sometimes higher n numbers) and large ELMs dominate the final collapse phase.

The high $\langle\beta_t\rangle$ regime is produced principally by the *skin effect*, resulting from a rapid I_p rampup ($\dot{I}_p \sim 2.5$ MA/s) and shaping. Plasmas in this regime have a large indentation ($\iota \sim 0.28$), ellipticity ($\kappa \sim 2.2$)

[4] The β collapse is a process discovered in the predecessor PBX tokamak [24, 2, 25], and has since been observed in many tokamaks including PBX-M.

and triangularity ($\delta \sim 0.60$). These L-mode, high I_p (~ 570 kA) discharges are characterized by a high $\langle\beta_t\rangle$ value ($\leq 6.8\%$), β_{TS} (~ 2 MA/m·T) and g factor ($g \sim 3.4\% \cdot m \cdot T/MA$). They possess a long MHD quiescent period (~ 100 ms) followed by a brief period (~ 30 ms) of global MHD activity before a disruption that terminates the discharge. The MHD activity has predominantly $n = 1$ and odd poloidal mode number m, and is similar to precursor oscillations before a sawtooth crash. It appears that the discharge terminates at, or just after, a sawtooth crash. The plasmas in this regime are entirely in the first stability region, but have the advantage of quiescent MHD and high confinement time usually associated with high I_p. They have the important disadvatange of ending inevitably in a disruption as q at the plasma edge becomes too low.

The pellet regime [27] is produced by modifying what would have been a typical high β_p regime discharge by injecting a centrally penetrating, medium sized (diameter to length ratio D/L ~ 2/3 mm) deuterium pellet. Pellets cause an H- to L-mode transition, and the subsequent equilibrium evolves differently from that of target H-mode plasmas without pellets. The plasmas produced by high density ($n_e(0) \leq 1.5 \times 10^{19}$ m^{-3}) pellets are characterized by a sustained (≥ 100 ms) peaked density profile and a long MHD quiescent period (≥ 80 ms), followed by a brief period (~ 30 ms) of MHD activity before a sawtooth crash or disruption. They have a quasi-steady I_p and high energy confinement time usually associated with high n_e, and have the potential to reach high β_p and second stability without suffering a β collapse (see below). The confinement time ($\tau_E \sim 45$ ms) is comparable to, or better than, that of the target H-mode discharges, in spite of profiles characteristic of the L-mode. Such a high confinement time is often associated with discharges with a high n_e or peaked n_e profile. The pellet regime discharges are similar to high $\langle\beta_t\rangle$ regime discharges in some ways, but also possess properties unattainable in the latter regime, such as very high densities and quasi-steady I_p.

4. PROFILES CREATED BY PROFILE MODIFICATION TOOLS

We reconstruct the current profile by obtaining a solution to the Grad–Shafranov equation using the FQ code (a version of the PEST code [28]) that matches observed magnetic measurements and uses a prescribed pressure profile constructed from Thomson scattering data. The magnetic measurements used as 'boundary conditions' in the reconstruction are the plasma and coil currents and two poloidal flux differences. The total pressure is assumed to be proportional to the electron pressure. It is also assumed in these calculations that $q(0) = 0.7$–0.9, partly chosen on the basis of a good fit between the measured and calculated pressure profiles. The assumed functional forms of pressure and toroidal field functions in the Grad–Shafranov equation ensure that the pressure gradient and the toroidal current density vanish on the plasma boundary.

The normalized profiles of pressure and current density along the B field lines, j_{ohm}, as a function of the normalized poloidal flux function, are compared in Fig. 2(a) and (b), respectively, for plasmas created with

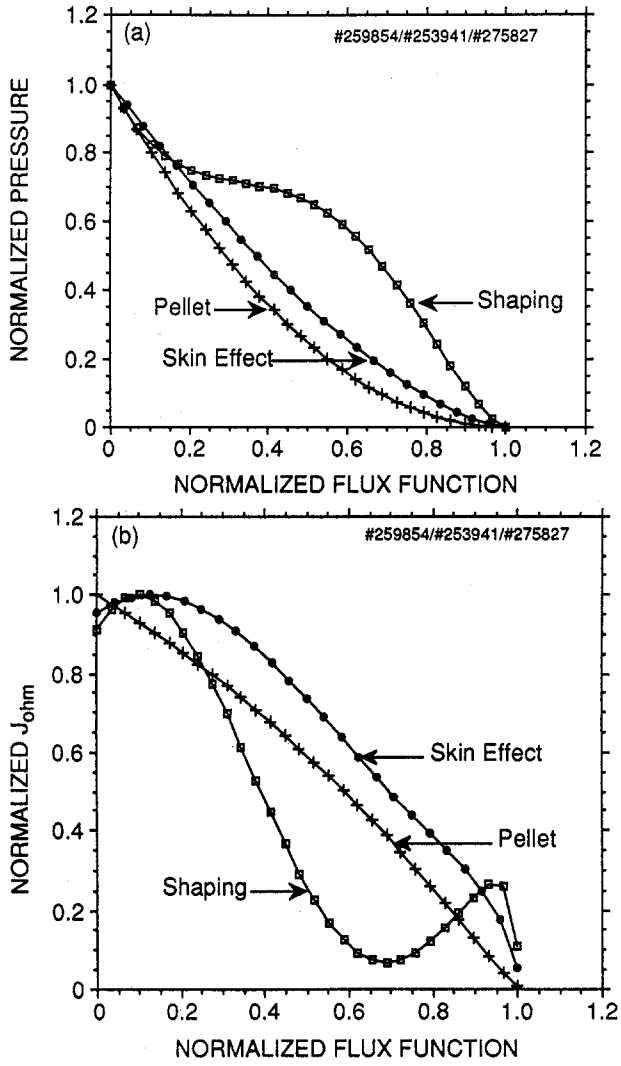

FIG. 2. Normalized profiles of (a) pressure and (b) current generated by three different profile modification tools: shaping, skin effect and pellet injection (the shot numbers are given in this order).

shaping alone (high β_p regime), with a strong skin effect (high $\langle\beta_t\rangle$ regime) and with pellet injection. The plasmas generated by shaping alone have a combination of a 'narrow' current profile ($\ell_i = 0.62$)[5] and a 'broad' pressure profile ($p_f = 2.5$). The current profile exhibits a 'double hump', consisting of a narrow central peak and a secondary peak near the plasma edge. The plasmas created by a strong skin effect have a combination of a broad current profile ($\ell_i = 0.45$) and a narrow pressure profile ($p_f = 3.0$). The plasmas created by pellet injection have a combination of a narrow current profile ($\ell_i = 0.73$) and a narrow pressure profile ($p_f = 3.8$).

Two contrasting equilibria are depicted in the S–α map in Fig. 1. Curves (A) and (B) in this figure are typical for high β_p and high $\langle\beta_t\rangle$ regimes, respectively. The pattern of trajectory (A) is first up (increasing S), then to the right (increasing α), and finally downward. The shear is often considered important for the MHD stability, but, for a monotonically varying q profile, the total amount of shear within the plasma is given when q values are specified at the plasma edge and the magnetic axis. The upward segment of the trajectory near the magnetic axis (up to, say, $q \leq 1$ for this case) implies expending a limited 'supply' of shear at places where there is no significant pressure gradient. The downward loop of trajectory (A) (beyond the $q = 3$ surface for this case) corresponds to diminishing shear, where the pressure gradient becomes large and is likely to contribute unfavourably to the kink stability. The downward loop is a characteristic feature of the S–α trajectory for H-mode plasmas with high β_p in the PBX-M tokamak. Associated with such a topological feature of the curve is the MHD-active nature of the plasma. Equilibria similar to that represented by trajectory (A) have been subjected to theoretical stability analysis [23, 29]. They were found to possess some ballooning unstable interior surfaces, generally in regions approximately delineated by $2 \leq q \leq 3$. But the quantitative relationship of the equilibrium trajectory to stability boundaries and hence the extent of the unstable region varied, depending upon parameters used in the equilibrium calculations, some of which were not well known. The equilibria were also found to be unstable to the external kink mode when the conducting walls are postulated at 1.5 times the plasma minor 'radius'.

In contrast, trajectory (B) in Fig. 1 first heads towards the right (increasing α) and then upward (increasing S). The pressure gradient increases near the magnetic axis (within the $q = 1$ surface for this case) while the shear remains low. If the objective of profile modification is to avoid high-n ballooning instability and to reach the second stability region, the topology of this trajectory appears promising. The trajectory pattern, if extended farther to the right (for example through heating), would be more likely to go under the ballooning stability boundary and thereby obtain second stability. The condition $q(0) > 1$, which is often considered desirable for achieving second stability, would produce a nearly shearless central region (for a given, moderate q at the plasma edge) and would let the trajectory pass safely under unstable zones, provided there is a finite pressure gradient there. Rapidly increasing shear near the edge should be favourable for kink stability. Equilibria similar to that represented by trajectory (B) have been subjected to theoretical stability analysis [23, 29] and were found to be stable against ballooning modes, and either stable or marginally stable for n = 1–3 kink modes, depending upon how the conducting walls are modelled.

The high β_p regime discharges have a quasi-steady-state plasma current, but are MHD active and often suffer a β collapse, while high $\langle\beta_t\rangle$ regime discharges are MHD quiescent, but are transient and suffer an inevitable low-q disruption. A third discharge regime produced with pellet injection may be capable of combining the quasi-steady-state and the MHD quiescent characteristics.

A pellet regime plasma is produced by injecting a pellet, during the β rise phase, into a discharge which would have evolved into a high β_p plasma in the absence of the pellet. By the time of injection, a double hump feature in the current profile, characteristic of a high β_p plasma, has formed to some extent in the target H-mode plasma, but the pressure profile has not yet broadened as much as that in a fully developed high β_p plasma (see Fig. 2). (Injection occurs in a state between those represented by curves (A) and (B) in Figs 4 or 5 shown below.) The pellet destroys the double hump in the current profile and brings the profile closer to that of an L-mode plasma produced by the skin effect. The pellet also prevents formation of a broad pressure profile characteristic of a high β_p plasma. The MHD activity, observed in the target H-mode plasma, is nearly absent for a long period after pellet injection. The normalized pressure and current profiles long ($\sim$63 ms) after injection of a pellet are shown in Figs 2(a) and (b), respectively. The electron temperature profile measured after pellet injection, as well as the computed current profile, possess characteristics of an L-mode plasma. The energy confinement time, however, remains as high

[5] The dimensionless internal inductance used in this paper is defined by $\ell_i \equiv (4/\mu_0 R_g I_p^2) \int dV B_p^2/(2\mu_0)$, where B_p is the poloidal magnetic field and R_g is the major radius of the plasma geometrical centre.

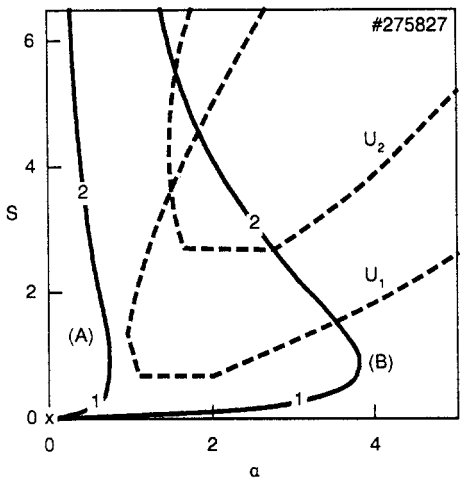

FIG. 3. The equilibrium of a discharge produced by pellet injection is represented by (A). The broken curves U_1 and U_2 are representative ballooning stability boundaries of the pellet produced equilibrium (for flux surfaces with q = 1.3 and 2.4, respectively). We hope to heat this plasma to higher pressures and to transform the equilibrium trajectory to a shape resembling the curve labelled (B) using profile modification tools.

as, or higher than, that of the target H-mode plasma, presumably because the pellet produced density is significantly higher than the target plasma density and also the pellet produced density profile is highly peaked. Increased confinement time has often been associated with high density and peaked density profiles in many tokamaks.

The equilibrium of a pellet discharge is depicted in the S–α map by trajectory (A) in Fig. 3. High-n ballooning stability boundaries, U_1 and U_2, are also shown in the figure for representative flux surfaces of the equilibrium with q = 1.3 and 2.4, respectively. Like a high β_p plasma, a pellet generated plasma contains a large amount of stored energy, yet, unlike a high β_p plasma, a pellet plasma is MHD quiescent and free from the β collapse. The trajectory of a pellet plasma, like that of a high $\langle\beta_t\rangle$ plasma, has low shear values in the central region ($q \leq 1$ for the case shown in the figure). Yet, unlike a high $\langle\beta_t\rangle$ plasma, a pellet plasma has a quasi-steady I_p and does not necessarily end with a low-q disruption. The state produced by injecting pellets into a high β_p plasma has not been achieved in any other way in PBX-M and appears to be a good starting point to access the second stability through heating of the central region while keeping the current profile substantially unchanged. A topologically similar trajectory (trajectory (B) in Fig. 3) that has a larger pressure gradient in the central low-shear region than

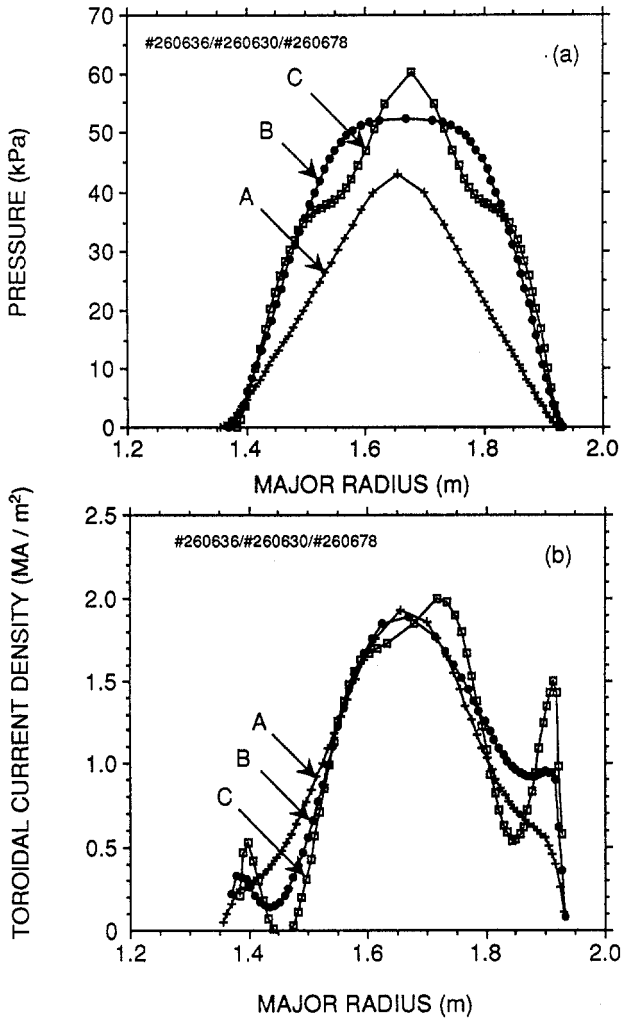

FIG. 4. Profile evolution of (a) pressure and (b) toroidal current density in β collapse discharges: in the early β rise phase (A), near the end of the rise phase (B) and near the β peak, just before the collapse phase (C).

trajectory (A) might represent a target state of our future experiments. In fact, an earlier study [16] of PBX-M plasmas showed that the main factor in determining access to the second stable regime is sufficient lowering of shear on each flux surface[6].

5. PROFILE CHANGES WITH β COLLAPSE AND AN ELM EVENT

In Section 4, equilibria at a specific time point during the discharge were compared for different regimes. In this section we examine the time evolution of the S–α

[6] The study cited here used different definitions of S and α, making a direct comparison of the equilibrium trajectories difficult.

pattern in the β collapse process. The high β_p state discussed earlier is often reached near the β_p peak or saturation in β collapse discharges. In addition, we will discuss abrupt changes in the S–α trajectory at an ELM event [29], which occurs frequently during the final phase of the β collapse process.

In Fig. 4(a) the pressure profile along the midplane major radius is shown for a sequence of three time points (from three similar discharges) during the initial part of a 'β collapse discharge', up to the β peak or saturation phase, but before the final collapse phase. During most of the β rise phase (up to about 420 ms in this series of discharges), a 'peaked' pressure profile ($p_f > 3$) is maintained. A representative profile is given by curve (A) (with $p_f = 3.8$ at 360 ms) during this period. Near the end of the rise phase, the pressure profile broadens strongly, as shown by curve (B) (with $p_f = 2.4$ at 450 ms). Near the β peak, just before the onset of the collapse phase, the pressure gradient in the peripheral regions steepens further, as shown by curve (C) (although $p_f = 3.4$ at 490 ms because of a higher peak pressure). Development of a 'shoulder' in the profile may have been caused by some MHD activity, probably ELMs, which began to appear by this time, but could also represent shot-to-shot variations. The profile at this time point, containing a large amount of stored energy, collapses to more peaked shapes and lower central pressures (not shown) in the final phase. In Fig. 4(b) the toroidal current profile along the midplane major radius is shown for the same set of discharges. The current profile, measured in terms of ℓ_i, broadens during the rise and saturation phases, from 0.73 to 0.62 to 0.53. But a prominent feature of the toroidal current evolution is the development of a double humped profile with an accompanying sharp edge gradient. The relationship between the pressure and current profiles may be seen better in an S–α map.

The equilibria in the same set of three time points during the β collapse process are represented in Fig. 5 in an S–α map. In this sequence, q_{95} (q value on the flux surface containing 95% of the difference in the poloidal flux between its values at the magnetic axis and the last closed magnetic surface) varies from 6.4 to 4.7 to 4.4, indicating a diminishing total available shear as β rises. Trajectory (C) shows a characteristic downward loop with a large increase in pressure gradient, yet no accompanying increase in the shear on flux surfaces beyond the q = 2 surface. The collapse phase begins after this state, and the stored energy decreases in spite of a steady power input from NBI. During this phase, a series of ELM events (a sudden drop of stored energy, probably caused by a short ($\leq$ 1 ms) burst of MHD activity) and continuous global (n = 1–3) MHD modes are observed. The downward loop is a combined result of a strong double hump in the current profile and a large pressure gradient near the plasma edge (see Fig. 4). A double hump alone does not necessarily form a downward loop.

The equilibria just before, and just after, an ELM event are shown in an S–α map in Fig. 6. The major effect of the ELM on the equilibrium appears on flux

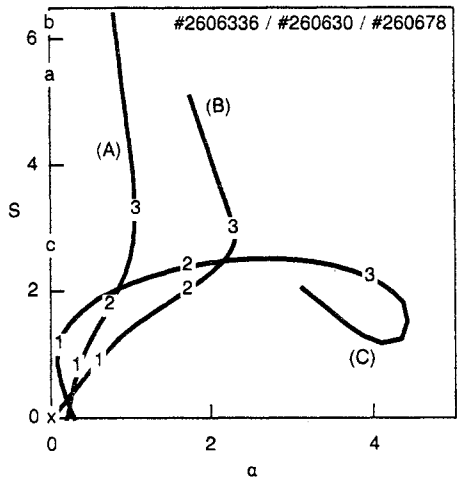

FIG. 5. Trajectory evolution in β collapse discharges: in the early β rise phase (A), near the end of the rise phase (B) and near the β peak, just before the collapse phase (C).

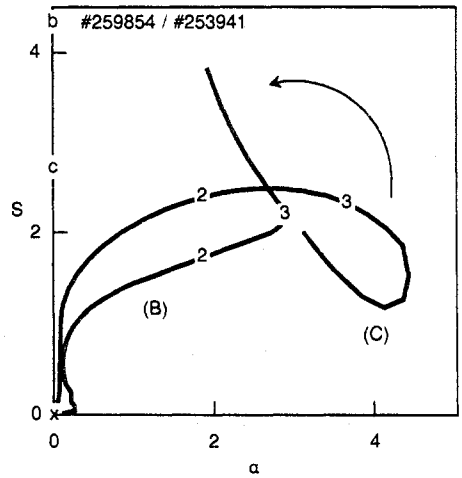

FIG. 6. Trajectories just before (C) and just after (B) a large ELM event. The ELM unravels the downward loop of trajectory (C) and flips it upward into regions of lower pressure gradient and higher shear. The resultant trajectory resembles the trajectory at the end of the rise phase (see trajectory (B) in Fig. 5).

surfaces beyond the q = 3 surface for this case. The ELM unravels the downward loop of trajectory (C) and flips it upward into a region of higher shear and reduced pressure gradient. The resultant trajectory (B), which resembles closely the trajectory at the end of the rise phase (see trajectory (B) in Fig. 5), may represent a transition from an unfavourable state to a favourable state for the stability of an MHD mode, possibly a kink mode. From a stability analysis [29] of a similar event, the equilibria, just before and just after an ELM event, were both found to be unstable for the external kink mode in the absence of conducting walls. The equilibrium just before the event required the walls to be much closer to the plasma, for the mode to be stabilized, than the equilibrium just after the event. From this quantitative analysis, the authors of the study drew the highly qualitative conclusion that changes in the equilibrium at the ELM event were in the direction of stability, i.e. from a less stable state to a more stable state.

In the final phase of β collapse discharges the stored energy often decreases in a step-like manner punctuated by the ELM events, recovering partially between two successive events. A downward loop presumably forms after the recovery in each step. The state represented by a downward loop in the S-α map appears to be unsustainable and is relieved by ELMs to yield a more stable configuration. The value of q_{95}, which is an approximate measure of the total available shear, is unaffected in the ELM event discussed here and, therefore, an increase in the shear in outer regions would require a compensating decrease elsewhere in core regions, as is evident in Fig. 6.

6. SUMMARY

Use of the S-α diagram is proposed as a method for characterizing plasma equilibria. It can provide more useful information than individual current and pressure profiles and their integral moments (for example, internal inductance and pressure peaking factor). The S-α map visually represents the *local variations* and the *interrelationship* between two important factors influencing the stability, namely the shear and the dimensionless pressure gradient. Through accumulated experience, both experimental and theoretical, it may be possible to discern from the trajectory pattern in the S-α map a qualitative measure of stability characteristics of an equilibrium, which may be more useful under practical circumstances than a simple statement that the equilibrium is, or is not, stable against a particular MHD mode. It is also worth while to explore whether any association can be found between the trajectory pattern and the confinement characteristics. (However, no examples have been offered from PBX-M experiments in this regard.)

The relative merit of equilibrium profiles may be discerned more easily through 'pattern recognition' in the S-α map than through examinations of current and pressure profiles individually. An equilibrium trajectory pattern in the diagram may be associated with a set of experimentally observed phenomena in the discharge represented by the equilibrium, such as the level and kind of MHD activity, and theoretically predicted stability or confinement. When qualitatively or topologically distinguishable trajectory patterns can be recognized as being associated with a different set of observable or predicted characteristics, the diagram will serve as a tool for cataloguing the presently achievable plasma states as well as ideal target states. Furthermore, types of changes that are produced by various profile modification techniques can also be represented in the same diagram. This can be used to help construct a desired equilibrium state, starting from a given experimental state and using profile modification techniques. The S-α map enables comparisons of equilibria from different devices independent of the plasma shape and size. In such comparisons the plasma shaping ability of a device is implicit as an available technique to alter the S-α pattern.

It has been demonstrated, using PBX-M experiments as examples, that qualitatively distinguishable trajectory patterns are associated with operational regimes having different MHD characteristics, and that some profile modification techniques and types of MHD activity produce characteristic trajectory changes. The high β_p and high $\langle\beta_t\rangle$ regimes, using shaping and rapid current ramp, respectively, are found to have different S-α patterns. The trajectory of the quasi-steady I_p, but MHD active, high β_p plasmas has characteristics qualitatively unfavourable both to the ballooning stability and the kink stability. In particular, the trajectory with a downward loop represents an unsustainable state and marks the onset of a final collapse in the β collapse process. The trajectory of the MHD quiescent, high $\langle\beta_t\rangle$ plasmas has qualitatively favourable stability characteristics, but the discharges are inherently transient and inevitably end in a low-q disruption. Pellet injection into a quasi-steady I_p, H-mode discharge, which would have evolved into a high β_p plasma in the absence of pellets, produces an L-mode plasma with a large amount of stored energy and an S-α trajectory similar to that of a high $\langle\beta_t\rangle$ plasma. The pellet plasma has the potential to combine the advantages of both regimes: a quasi-steady state and

an MHD quiescent state. It may serve as a good starting state for accessing the second stable regime.

The time evolution of the equilibrium in a β collapse discharge, up to a high β_p plasma state near the β peak, also manifests itself as a series of characteristic changes in the S–α trajectory, ending in the formation of a downward loop. A prominent change in the trajectory caused by the ELM event, which occurs frequently in the final collapse phase of the β collapse process, is unravelling of the downward loop, and results in a trajectory with higher shear and lower pressure gradient, which is presumably more favourable for the kink stability.

ACKNOWLEDGEMENTS

The authors wish to acknowledge contributions from R. Hatcher to this work. They would also like to thank other members of the PBX-M group for their support of this work.

The PBX-M project is supported by the United States Department of Energy, under Contract No. DE-AC02-76-CHO-3073.

REFERENCES

[1] STAMBAUGH, R.D., MOORE, R.W., BERNARD, L.C., et al., in Plasma Physics and Controlled Nuclear Fusion Research 1984 (Proc. 10th Int. Conf. London, 1984), Vol. 1, IAEA, Vienna (1985) 217.

[2] OKABAYASHI, M., BOL, K., CHANCE, M.S., et al., in Plasma Physics and Controlled Nuclear Fusion Research 1986 (Proc. 11th Int. Conf. Kyoto, 1986), Vol. 1, IAEA, Vienna (1987) 275.

[3] BOL, K., BUCHENAUER, D., CHANCE, M., et al., Phys. Rev. Lett. **57** (1986) 1891.

[4] ZARNSTORFF, M., BARNES, C.W., EFTHIMION, P.C., et al., in Plasma Physics and Controlled Nuclear Fusion Research 1990 (Proc. 13th Int. Conf. Washington, DC, 1990), Vol. 1, IAEA, Vienna (1991) 109.

[5] NAVRATIL, G.A., GROSS, R.A., MAUEL, M.E., et al., ibid., p. 209.

[6] SABBAGH, S.A., GROSS, R.A., MAUEL, M.E., et al., Phys. Fluids B **3** (1991) 2277.

[7] ZARNSTORFF, M.C., BELL, M.G., BITTER, M., et al., Phys. Rev. Lett. **60** (1988) 1306.

[8] KIKUCHI, M., AZUMI, M., TSUJI, S., TANI, K., KUBO, H., Nucl. Fusion **30** (1990) 343.

[9] KAUFMANN, M., BÜCHL, K., FUSSMANN, G., et al., Nucl. Fusion **28** (1988) 827.

[10] ONO, M., in Applications of Radiofrequency Power to Plasmas (Proc. 7th Top. Conf. Kissimee, FL, 1987), American Institute of Physics, New York (1987) 230.

[11] FISCH, N., Rev. Mod. Phys. **59** (1987) 175.

[12] MOREAU, D., GORMEZANO, C., Plasma Phys. Control. Fusion **33** (1991) 1621.

[13] SYKES, A., TURNER, M.F., in Controlled Fusion and Plasma Physics (Proc. 9th Eur. Conf. Oxford, 1979), Vol. 1, UKAEA, Culham Laboratory, Abingdon, Oxfordshire (1979) 161.

[14] COPPI, B., CREW, G.B., RAMOS, J.J., Comments Plasma Phys. Control. Fusion **8** (1983) 11 (Fig. 2).

[15] FU, G.Y., Van DAM, J.W., ROSENBLUTH, M.N., Nucl. Fusion **29** (1989) 1939.

[16] PHILLIPS, M.W., HUGHES, M.H., TODD, A.M.M., OKABAYASHI, M., KAYE, S.M., LeBLANC, B., Phys. Fluids B **2** (1990) 973.

[17] TROYON, F., GRUBER, R., SAURENMANN, H., SEMENZATO, S., SUCCI, S., Plasma Phys. Control. Fusion **26** (1984) 209.

[18] POST, D.E., BORRASS, K., CALLEN, J.D., et al., in ITER Documentation Series, No. 21, IAEA, Vienna (1991) Sect. 2.2.

[19] SAUTHOFF, N., ASAKURA, N., BELL, R., et al., in Plasma Physics and Controlled Nuclear Fusion Research 1990 (Proc. 13th Int. Conf. Washington, DC, 1990), Vol. 1, IAEA, Vienna (1991) 709.

[20] CONNOR, J.W., HASTIE, R.J., TAYLOR, J.B., Phys. Rev. Lett. **40** (1978) 396.

[21] CHANCE, M.S., in Theory of Fusion Plasmas (Proc. Workshop Varenna, 1987), Editrice Compositori Bologna (1988) 87.

[22] LUXON, J.L., BRAMSON, G., BURRELL, K.H., et al., Plasma Phys. Control. Fusion **32** (1990) 869.

[23] BELL, R., ASAKURA, N., BERNABEI, S., et al., Phys. Fluids B **2** (1990) 1271.

[24] TAKAHASHI, H., BOL, K., BUCHENAUER, D., et al., in Controlled Fusion and Plasma Physics (Proc. 12th Eur. Conf. Budapest, 1985), Vol. 9F, Part I, European Physical Society (1985) 58.

[25] KUGEL, H., SESNIC, S., BOL, K., et al., in Controlled Fusion and Plasma Physics (Proc. 14th Eur. Conf. Madrid, 1987), Vol. 11D, Part I, European Physical Society (1987) 185.

[26] KEILHACKER, M., BECKER, G., BERNHARD, K., et al., Plasma Phys. Control. Fusion **26** (1984) 49.

[27] TAKAHASHI, H., BELL, R., CHANCE, M.S., et al., paper 5Q4, presented at 31st Annual Meeting of Division of Plasma Physics, American Physical Society, Anaheim, CA, 13–17 Nov. 1989.

[28] JOHNSON, J.L., DALHED, H.E., GREENE, J.M., et al., J. Comput. Phys. **32** (1979) 212.

[29] KAYE, S.M., MANICKAM, J., ASAKURA, N., et al., Nucl. Fusion **30** (1990) 2621.

(Manuscript received 25 February 1991
Final manuscript received 29 January 1992)